Hindawi Publishing Corporation
International Journal of Vehicular Technology
Volume 2015, Article ID 670482, 10 pages
http://dx.doi.org/10.1155/2015/670482

Research Article

Channel Impulse Response Estimation in IEEE 802.11p via Data Fusion and MMSE Estimator

Giulio Ministeri and Lorenzo Vangelista

Department of Information Engineering, University of Padova, Via Gradenigo 6/B, 35131 Padova, Italy

Correspondence should be addressed to Giulio Ministeri; minister@dei.unipd.it

Received 19 December 2014; Revised 4 March 2015; Accepted 4 March 2015

Academic Editor: Martin Reisslein

Tracking the channel impulse response in systems based on the IEEE 802.11p standard, the most widely accepted standard for the physical layer in vehicular area networks (VANETs), is still an open research topic. In this paper we aim to improve previously proposed channel estimators by utilizing data aided algorithm that includes the channel decoding to enhance the quality of the estimated data. Moreover we propose a novel technique that exploits information provided by external sensors like GPS or speedometer, usually present in vehicles. The algorithm proposed so far has been analyzed in non-line-of-sight link conditions; in this paper we present an analysis of performances in the line-of-sight condition as well. Simulations show that both proposals give considerable improvements in terms of packet error rate and channel estimation error in the highway scenario which is surely the most stressing environment for the channel response tracker.

1. Introduction

Vehicular ad hoc networks (VANETs) aim at improving safety in vehicular transportation systems; new cars will be equipped with devices capable of sharing information, through wireless links, about the current status, preventing collisions and alarming drivers of incoming hazardous situations. However, VANETs mean not only safety but also connectivity and Internet access for a wide range of onboard applications known as infotainment, that is, information for improving traffic efficiency and entertainment for drivers and passengers.

The most common VANET physical layer, also known as DSRC (direct short range communications), is based on the IEEE 802.11p standard [1, 2]; it uses an orthogonal frequency division multiplexing (OFDM) transmission, and thanks to different symbol modulations and code puncturing schemes it allows the transmission to occur at different rates, ranging from 3 to 27 Mb/s.

As well known, for the performances of any OFDM receiver the channel estimation is critical. However, since the IEEE 802.11p standard inherits most of its features from the well known IEEE 802.11a standard for wireless local area networks, it does not provide sufficient information (e.g., pilot tones) for the purpose of channel tracking. In IEEE 802.11a, wireless links are typically created between an access point, always considered in a static position, and terminals, which are assumed to have very slow speed, at most 15 km/h, and nomadic behaviors, that is, stationary for most of the time. In VANETs terminals are seldom stationary, and they can have a very wide range of speeds, from few km/h in metropolitan areas up to 150 km/h in highways. As showed in many papers [3, 4], receiver schemes used for WLANs poorly fit VANETs: higher speed of terminals leads to shorter coherence time of the channel so the initial channel response (CR) estimate is valid for a much shorter period.

Furthermore the outdoor scenario of VANETs is in contrast with the typical indoor environment for which the wireless local area networks have been designed: as already pointed out, the coherence bandwidth of the channel is smaller and the pilot tones are too few and too far (in the frequency domain) from each other to enable an adequate channel estimation and tracking.

But as we focus our receiver design for VANET-specific devices we can get many advantages: as suggested in the standard, the VANET devices will likely be equipped with

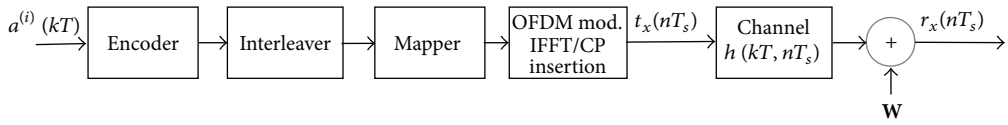

Figure 1: IEEE 802.11p reference system model.

a GPS sensor to acquire universal time reference; moreover, for safety purposes, they should have direct links with in-car sensors and electronic control units.

In this paper we firstly cope with the problem of pilot tones deficiencies by using a parametric channel model and the least square error estimator in the CR estimation process. We then aim to improve the channel tracking process by exploiting information from the in-car sensors and improve the efficiency of the OFDM receiver; in particular we try and estimate the Doppler effect from the information on vehicle speed provided by GPS or speedometer sensors. We focused on road to vehicle (RTV) in highway scenario where vehicle speed and Doppler effect have a more direct relationship and we show that considerable improvements in terms of receiver efficiency can be obtained.

2. System Model

The IEEE 802.11p protocol physical layer is a frame-based OFDM transmission with $N = 64$ subcarriers and a cyclic prefix (CP) of length $N_{\mathrm{CP}} = 16$.

To mitigate the Doppler effects due to the fast-moving environment the bandwidth has been halved (with regard to IEEE 802.11a) to $B = 10\,\mathrm{MHz}$; thus the sampling period is $T_s = 1/B = 6.4\,\mu\mathrm{s}$ and the OFDM symbol time period is $T = (N + N_{\mathrm{CP}})T_s = 8\,\mu\mathrm{s}$.

The frame structure is presented in Figures 2 and 3: every frame starts with a sequence of fixed symbols; the tenfold repetition of the short sequence $\mathbf{t}_i, i = 1, \ldots, 10, \mathbf{t}_i \triangleq \mathbf{t}_s$, is used by the receiver to detect the frame, while the long sequence symbols $\mathbf{T}_1 = \mathbf{T}_2 \triangleq \mathbf{T}_L$ are used by the receiver to perform channel response estimation (CRE).

The IEEE 802.11p transmitter is presented in Figure 1: the convolutional encoder with constraint length L_{CC}, the interleaver, and the symbol modulator have different configurations to allow different transmission rates [1].

In our model the received signal is obtained by filtering the transmitted signal $t_x(nT_s)$ with the time-varying channel impulse response (CIR) $h(kT, nT_s)$ and adding white Gaussian noise (WGN) with statistical power such that the signal to noise ratio (SNR) equals

$$\mathrm{SNR} = \frac{P_{tx}}{\sigma_w^2}. \tag{1}$$

We focus in the case where perfect time and frequency synchronization between transmitter and receiver is already achieved; we also assume the time-varying CIR to last no more than the CP time:

$$nT_s \geq N_{\mathrm{CP}}T_s \Longrightarrow h\left(kT, nT_s\right) = 0, \quad \forall k > 0. \tag{2}$$

In this case, neglecting changes in the $h(kT, nT_s)$ during the symbol reception, the OFDM demodulated signal can be expressed in the frequency domain as

$$\mathbf{Y}(k) = \mathbf{H}(k) \cdot \mathbf{X}(k) + \mathbf{W}(k), \tag{3}$$

where $\mathbf{H}(k)$ is the discrete Fourier transform (DFT) of the N-element vector $\mathbf{h}(k)$ which is the sampled CIR $h(t, nT_s)$ $n = 1, \ldots, N$ at the time instant kT; $\mathbf{X}(k)$ is an $N \times N$ diagonal matrix with data symbols $a^{(i)}(k)$ in its diagonal and $\mathbf{W}(k)$ is the additive noise vector.

The most common CRE algorithm is based on least square estimation (LSE): the long training sequence symbols $\mathbf{T}_1$ and $\mathbf{T}_2$ can be expressed as

$$\mathbf{Y}_{\mathbf{T}_1} = \mathbf{H}(0) \cdot \mathbf{X}_{\mathbf{T}_1}, \qquad \mathbf{Y}_{\mathbf{T}_2} = \mathbf{H}(2) \cdot \mathbf{X}_{\mathbf{T}_2} \tag{4}$$

and, applying the zero-forcing criterion [5, page 776] the channel response is estimated as

$$\widehat{\mathbf{H}}(0) = \frac{1}{2}\left(\mathbf{Y}_{\mathbf{T}_1} + \mathbf{Y}_{\mathbf{T}_2}\right) \cdot \mathbf{X}_{\mathbf{T}_L}^{-1}. \tag{5}$$

As mentioned before, in WLANs, receivers use $\widehat{\mathbf{H}}(0)$ to equalize the whole frame, since the CR can be assumed to be constant for the entire frame reception time.

The header symbol denoted in Figures 2 and 3 with the name SIGNAL contains information on the frame length, modulation, and coding schemes used in the subsequent payload symbols; it is encoded with the most robust code and modulated using BPSK constellation. The receiver must decode and parse this information before starting to decode the first payload symbol.

In Figure 3 the entire IEEE 802.11p frame structure is shown. Within the payload symbols, $L_{\mathrm{pp}} = 4$ subcarriers are filled with a predefined sequence of pilot symbols $p_i(k)$ $i = 1, \ldots, L_{\mathrm{pp}}$. The purpose of these symbols is to track drifts in the receiver internal oscillator.

2.1. Channel Model. Many efforts have been made to characterize the vehicular channel in different scenarios and many models have been presented. In [6] the authors describe how to build a geometric and stochastic mixture model valid only for vehicle to vehicle (VTV) communications in highways scenario.

In this paper we use the model described in [7], where specific model parameters are described for several vehicular communication scenarios. The model is presented for single antenna systems; it is based on the tapped delay line with the WSSUS assumption, and the Doppler parameters are inferred from vehicles speed. We use the implementation provided in [8] built upon the IT++ framework [9] where

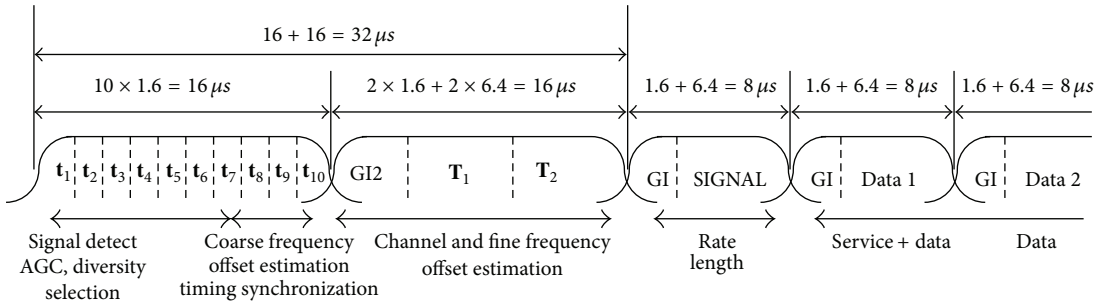

Figure 2: IEEE 802.11p frame structure.

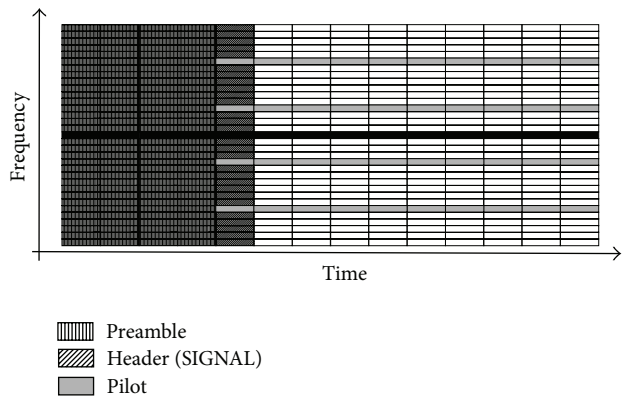

Figure 3: IEEE 802.11p frame structure in frequency and time domain.

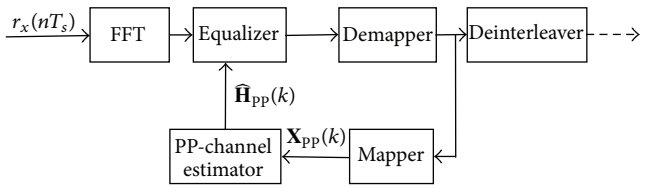

Figure 4: Pseudopilot channel estimation block scheme.

vehicles speed can be set. Hence, even if, in [7], models' parameters are provided for a specific vehicle speed and no real measurements support it, we think this is a reasonable method to simulate channels with different vehicle speed scenarios.

3. Related Works

Many channel tracking mechanisms have been proposed; most of them cope with the problem of channel estimation and tracking by proposing new transmission schemes.

In [10], authors suggest modifying the standard and adding a mid-amble OFDM symbol every M payload symbols (where M is fixed and depends on the modulation scheme), so the receiver can recompute the CRE periodically. Although it seems the most reasonable solution to the channel tracking problem, it introduces a strong modification to the standard which implies backward compatibility issues.

In [11] authors show the benefits given by a different approach to classical OFDM scheme, using the differential OFDM (DOFDM) transmission where the demodulation process does not need equalization any more. Assuming the channel impulse response to have small variations between subsequent OFDM symbols, data symbols are demodulated by taking the difference with the previous one in the same subcarrier. This approach shows good performances; however the authors do not explain the transition among the BPSK constellation of the header symbol and the subsequent symbols.

In [12] the authors propose a new algorithm based on the discrete prolate spheroidal (DPS) sequences. Knowing the channel characteristics, the domain of the CR can be tightened to a smaller subset, leading to the definition of a new transfer function whose model can be thought of as a convolutional code, iteratively decoded by a BCJR decoder [13]. Although this algorithm theoretically works whatever the frame structure, authors show that the current IEEE 802.11p preamble and pilot tones structures are not sufficient to let the decoder converge within a feasible time: the pilot tones distribution does not satisfy the sampling theorem condition, and thus the BCJR decoder must carry out a lot of iterations to reach satisfactory performances, forcing the system to very high computational efforts. Authors conclude by suggesting a backward compatible modification to the standard, which consists in adding a postamble symbol to the IEEE 802.11p frame, to be used to increase initial information for the decoding algorithm. Even if this solution can be seen as a backward compatible improvement of the standard, adding a postamble symbol increases transmission inefficiency.

Proposals which do not require modifications to the standard came up with the common idea to use data-aided pilot tones to solve the problem of the lack of pilot tones, the so-called pseudopilot tones (PP tones) construction. As in Figure 4, after the demodulator the OFDM symbols of the frame payload are brought back to the original values of the constellation and used to fill the $X_{PP}(k)$ matrix and assess the newer CR estimate with LS estimator:

$$\widehat{\mathbf{H}}_{PP}(k) = \mathbf{Y}(k) \cdot \mathbf{X}_{PP}^{-1}(k). \quad (6)$$

In [14] the authors propose the "channel smoothing" technique: exploiting (2) they use the truncated discrete Fourier transform DFT (DFT_{TR}) matrix to shrink the last coefficient

of the $\mathbf{h}(k)$ vector. $\widehat{\mathbf{H}}(k)$ is computed as a double Fourier transformation of the vector $\widehat{\mathbf{H}}_{\mathrm{PP}}(k)$:

$$\widehat{\mathbf{H}}(k) = \mathrm{DFT}\left[\mathrm{IDFT}_{\mathrm{TR}}\left(\widehat{\mathbf{H}}_{\mathrm{PP}}(k)\right)\right], \tag{7}$$

where $\mathrm{IDFT}_{\mathrm{TR}}$ is the truncated inverse DFT.

In [15] the correlation of the evolving CR is exploited to mitigate errors coming from the PP-tones algorithm and the hard symbol demodulation process. With an algorithm similar to the recursive least square filter, authors update the CR by averaging the old estimation with the newer one. To cope with the noise in low SNR conditions an extra cycle of frequency-domain averaging is made before the time-domain averaging step. They average the per-subchannel coefficients of the estimated CR with the adjacent ones:

$$\widehat{\mathbf{H}}_{up}^{(i)}(k) = \frac{1}{2\beta+1}\sum_{t=i-\beta}^{i+\beta}\widehat{\mathbf{H}}_{\mathrm{PP}}^{(t)}(k) \tag{8}$$

and then make the final step: the recursive average in the time domain

$$\widehat{\mathbf{H}}_{\mathrm{STA}}(k) = (1-\gamma)\,\widehat{\mathbf{H}}_{\mathrm{STA}}(k-1) + \gamma\widehat{\mathbf{H}}_{up}(k). \tag{9}$$

Since the averaging is made in both frequency and time domain, they call the method "spectral temporal averaging" (STA).

In [16] the authors present "constructed data pilot" (CDP) method, where a heuristic algorithm exploits the time correlation of the channel. The first CRE $\widehat{\mathbf{H}}_{\mathrm{CDP}}(0)$ is obtained by (5).

The subsequent CREs are computed by comparing the equalization results on the same received OFDM symbol $\mathbf{Y}(k)$ of the vectors $\widehat{\mathbf{H}}_{\mathrm{CDP}}(k-1)$ and the vector $\widehat{\mathbf{H}}_{\mathrm{PP}}(k)$ (6); if the demodulator decides for the same symbol in both cases then

$$\widehat{\mathbf{H}}_{\mathrm{CDP}}^{(i)}(k) = \widehat{\mathbf{H}}_{\mathrm{PP}}^{(i)}(k); \tag{10}$$

otherwise

$$\widehat{\mathbf{H}}_{\mathrm{CDP}}^{(i)}(k) = \widehat{\mathbf{H}}_{\mathrm{CDP}}^{(i)}(k-1). \tag{11}$$

The previously mentioned data-aided estimation algorithms are based on the demodulator performance which is heavily influenced by the SNR level of the received signal. The catastrophic effects due to errors in symbol demodulation bring the channel estimators to compute matrix $\mathbf{X}(k)$ with mistaken symbols, generating a wrong CRE, which, as a consequence, brings the symbol demodulator to make many errors in the next iteration.

We also noticed the complete absence of any consideration about the coherence time of the CR. In the STA algorithm the parameter γ is constant and independent of the vehicle speed, and the recursive estimation of the CRs intrinsically considers the channel to be time correlated even for infinite time lapses. In the CDP algorithm there is no theoretical analysis about the coherence time, and the time correlation is only implicitly exploited during the comparison of the equalization results.

4. Proposed Scheme

A first improvement to the aforementioned methods is to include the decoding and recoding steps in the cycle of pseudopilot channel estimation.

As well known the decoder introduces a delay which is at least equal to the constraint length of the transmitter encoder, so for every incoming OFDM symbol we only have at most the first $D = N - L_{\mathrm{CC}}$ symbols; the computation of the CR as in (6) then becomes impossible, since the matrix $\mathbf{X}(k)$ is only partially available, with uncertainties on the number and placements of the missing values.

As showed in [17] channel reconstruction techniques like spline or linear interpolation are error prone in case of wide spaced or not equally spaced pilot tones.

Thanks to sparse vector estimation and the algorithm described in [18], we can overcome this problem.

The expression (3) can be rewritten (omitting the additive noise) as

$$\mathbf{Y}(k) = \mathbf{X}(k)\cdot\mathbf{W}\cdot\mathbf{h}(k), \tag{12}$$

where vector $\mathbf{h}(k)$ has length L_{ch} and $\mathbf{W}$ is the $N \times L_{\mathrm{ch}}$ truncated DFT matrix. In fact, we fairly suppose the impulse response to have only the first L_{ch} coefficients to be nonnull as confirmed in [7, 19, 20] where the authors state that the vehicular CIR typically never last more than 1000 ns, (i.e., exactly 10 samples at 10 MHz sampling rate). So we remove the null coefficients from the $\mathbf{h}(k)$ vector and the last $N - L_{\mathrm{ch}}$ columns from the $\mathbf{W}$ DFT matrix.

We must also take into account the fact that the $\mathbf{X}(k)$ matrix contains only $D < N$ valid data, so we build the selection matrix $\mathbf{S}$ with dimension $D \times N$, which extracts the nonnull elements of the $\mathbf{X}(k)$ matrix. We rewrite (12) as

$$\overline{\mathbf{Y}} = \overline{\mathbf{X}}\cdot\overline{\mathbf{W}}\cdot\mathbf{h}, \tag{13}$$

where

$$\overline{\mathbf{Y}} = \mathbf{S}\cdot\mathbf{Y}, \qquad \overline{\mathbf{X}} = \mathbf{S}\cdot\mathbf{X}\cdot\mathbf{S}^{T}, \qquad \overline{\mathbf{W}} = \mathbf{S}\cdot\mathbf{W}. \tag{14}$$

If $D \geq L_{\mathrm{ch}}$, for every incoming OFDM symbol k, we can retrieve $\mathbf{h}(k)$ using the normal equation:

$$\hat{\mathbf{h}}(k) = \left[\left(\overline{\mathbf{X}}(k)\cdot\overline{\mathbf{W}}\right)^{H}\cdot\overline{\mathbf{X}}(k)\cdot\overline{\mathbf{W}}\right]^{-1}\cdot\left(\overline{\mathbf{X}}(k)\cdot\overline{\mathbf{W}}\right)^{H}\cdot\overline{\mathbf{Y}}(k). \tag{15}$$

And finally we obtain the CR estimation in the frequency domain as

$$\widehat{\mathbf{H}}(k) = \mathbf{W}\cdot\hat{\mathbf{h}}(k). \tag{16}$$

We called this modified version of the algorithm presented in [18] PP-MMSE to underline the fact that channel estimation is based on data-aided pilot tones also known as pseudopilot (PP) tones.

The condition

$$D \geq L_{\mathrm{ch}} \tag{17}$$

is a necessary condition; if not fulfilled the matrix

$$\mathbf{Z}(k) = \left(\overline{\mathbf{X}}(k) \cdot \overline{\mathbf{W}}\right)^{H} \cdot \overline{\mathbf{X}}(k) \cdot \overline{\mathbf{W}} \tag{18}$$

would not be full rank and it can not be inverted. $\mathbf{Z}(k)$ is also related to the variance of the estimation. The LS estimator theory [21, page 47] and the model parameters

$$\beta = \left(X^{H}X\right)^{-1} X^{H} y \tag{19}$$

have variance equal to

$$\operatorname{var}(\beta) = \sigma^{2}\left(X^{H}X\right)^{-1}, \tag{20}$$

where σ^2 is the noise variance and the matrix $(X^HX)^{-1}$ can be interpreted as the estimation of the covariance matrix of the input vector x, which, in our case, corresponds to the transmitting symbols. We can, thus, rewrite the final variance of the estimated parameters β as

$$\operatorname{var}(\beta) = \frac{\sigma^{2}}{N \operatorname{cov}(x)} \tag{21}$$

and conclude that, to reduce the variance and enhance the estimation reliability, we can only act on the number N of the input matrix X. This means, in practice, that the more the matrix X in (12) is close to be a full rank $N \times N$ matrix, the less the estimation error of the CR will be (16).

The choice of the trellis depth (depending on the constrained length of the code) of the Viterbi decoder must guarantee a number of valid symbols per OFDM frame $D \geq L_{CC} - L_{pp}$.

For every incoming OFDM symbol the receiver decodes the symbols with the extra Viterbi decoder and pads with zeroes the vector of length D to obtain the right dimension N; then data are reencoded and reinterleaved. Based on the interleaver shuffling pattern, the pilot construction block selects the subcarrier indexes which contain valid data. It also builds the DFT sparse matrix $\mathbf{W}$, used by the following block to compute the $\widehat{\mathbf{H}}(k)$ response according to (15) and (16).

As mentioned we also focus the receiver design on the VANET scenario and exploit further information about vehicle status to improve performances; in particular we are interested in the vehicle speed provided by GPS receiver to estimate the Doppler effects' parameters.

A nonzero speed between transmitter and receiver is the principal cause of Doppler effects, which gives rise to frequency shift and frequency broadening of the received signal [22, page 88]. The Doppler spectrum describes this phenomenon in terms of the probability density function (pdf) of the incident waves' magnitude at the different frequencies within the signal bandwidth. In case of non-line-of-sight (NLOS) communication, Rayleigh pdf is used and the relative Doppler spectrum is the well known Jakes' model:

$$D(f) = \begin{cases} \dfrac{1}{\pi f_D \sqrt{1 - \left(f/f_D\right)^2}}, & |f| \leq f_D, \\ 0, & \text{otherwise}, \end{cases} \tag{22}$$

where f_D is the maximum frequency of the Doppler spread. On the contrary if there exists a Dominant component the Rice process best suits the LOS communication scenario. Here we assume the communication to be in NLOS and we follow the procedure described in [23], where the authors approximate every tap Doppler spectrum with the Jakes model. Then we will show that, for our purposes, the error we are making in not considering a LOS communication is negligible.

From the Jakes spectrum the autocorrelation function of the channel impulse response in the continuous time domain is equal to [5, page 313]

$$r(\Delta t; \tau) = \int h(t, \tau)\, h^{*}(t + \Delta t, \tau)\, dt \tag{23}$$

$$= \sum_{n=1}^{L_{ch}} \sigma_{\tau_n}^{2} J_0\left(2\pi f_D \Delta t\right) \delta\left(\tau - \tau_l\right), \tag{24}$$

where $\sigma_{\tau_n}^2$ is the energy associated to a given delay τ_n and $J_0(x)$ is the zero-order Bessel function.

In the discrete time domain the CIR becomes

$$h_n(t) = h(t, nTs) \tag{25}$$

and the correlation function (23) becomes

$$r_{h_n}(\Delta t) = \sigma_{h_n}^{2} J_0\left(2\pi f_D \Delta t\right). \tag{26}$$

The difference between the tap coefficient at time t and at time $t + \Delta t$ is

$$\Delta h_n(\Delta t) = h_n(t) - h_n(t + \Delta t) \tag{27}$$

with statistical power equal to

$$E\left[\left\|\Delta h_n(\Delta t)\right\|^2\right] = 2\sigma_{h_n}^{2}\left(r_{h_n}(0) - r_{h_n}(\Delta t)\right). \tag{28}$$

Assuming the channel filter energy is equal to 1 we calculate the variance of the error we would make if we do not update the channel response for a certain number of OFDM symbols m:

$$\sigma_h^2(mT) = \sum_{l=0}^{L_{ch}} 2\left(r_{h_n}(0) - r_{h_n}(mT)\right) = 2\left(1 - J_0\left(2\pi f_D mT\right)\right). \tag{29}$$

Our key idea is to use the current vehicle speed to infer the f_D parameter by using the formula

$$f_D = f_c \frac{v}{c}, \tag{30}$$

where f_c is the carrier frequency, c is the speed of light, and v is the vehicle speed acquired from the GPS or in-car sensor. We also suppose that if we do not update the channel for a given number of symbols, we are implicitly considering the CR constant for that time period; thus we can fairly average the estimated CRs to reduce the estimation variance.

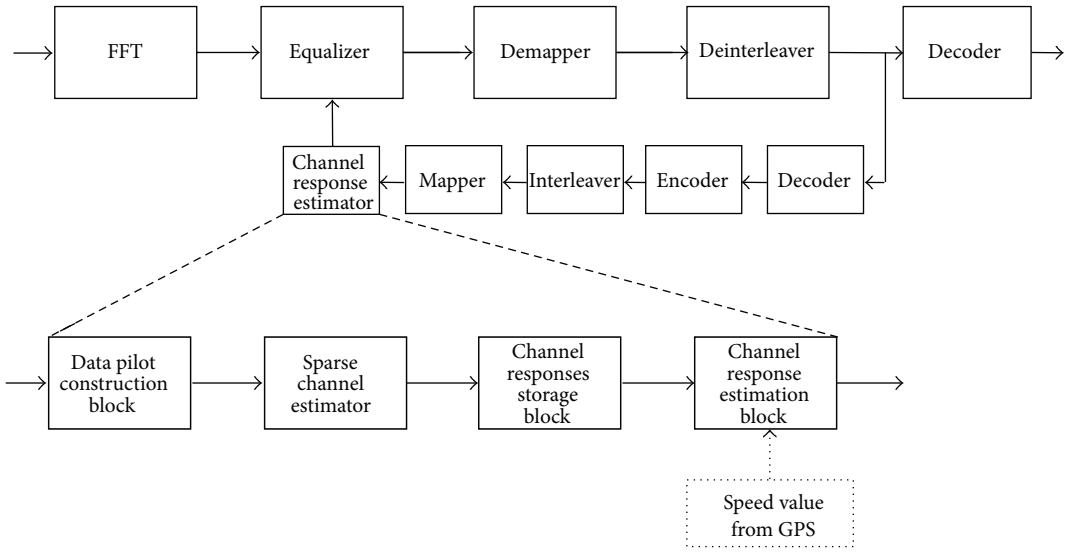

Figure 5: Structure of the proposed receiver.

We conclude that a time-averaging operation of subsequent CR estimations induces two opposite effects: reduction of the additive noise power and increase of the estimation variance due to CR changes. For a certain SNR level, we calculate the experienced SNR value eSNR as

$$\mathrm{eSNR}(m) = \frac{1}{(1/m)\left(1/\mathrm{SNR} + \sum_{k=1}^{m} \sigma_h^2(kT)\right)}. \quad (31)$$

In Figure 6 the eSNR with respect to real SNR is shown; for an update rate of $m = 1$, eSNR is almost equal to real SNR except for high SNR values where the channel variability within the single OFDM symbol is noticeable.

In practice, for every incoming frame our receiver estimates the SNR level from the long training sequence symbols as

$$\mathrm{SNR} = \frac{1}{2N} \sum_{n=1}^{N} \left\| Y_{T_1}^{(n)} - Y_{T_2}^{(n)} \right\|^2 \quad (32)$$

as explained in [24]; then using (31) with different value of m, it seeks for the best channel updating rates, that is, the updating rate which guarantees the highest value of the eSNR.

To analyze the case of a LOS communication we have first to change the per-tap autocorrelation function (26). The first coefficient h_1 includes a dominant component due to the LOS path and the Rice distribution should be used; (26) should be substituted with the formula in [25]

$$r_{h_n}(\Delta t) = \sigma_{h_n}^2 \frac{I_0\left(\sqrt{\kappa^2 - 4\pi^2 f_D^2 \Delta t^2 + j4\pi\kappa f_D \Delta t}\right)}{I_0(\kappa)}, \quad (33)$$

where κ represents the power ratio between the LOS components and the scatterers, and it is easy to show that, with $\kappa = 0$, (33) becomes (26). Taking the real part of the autocorrelation function (33) and following the same procedure as for the NLOS case, the final formula for the error variance (29) becomes

$$\sigma_h^2(mT) = 2\left[1 - \left(1 - \sigma_{h_1}^2\right) J_0(2\pi f_D mT)\right] - \sigma_{h_1}^2 \frac{I_0\left(\sqrt{\kappa^2 - 4\pi^2 f_D^2 \Delta t^2 + j4\pi\kappa f_D \Delta t}\right)}{I_0(\kappa)}, \quad (34)$$

where $\sigma_{h_1}^2$ is the fraction of the energy of the first tap with respect to the total channel energy. Finally if we substitute $\sigma_h^2(mT)$ in (31) we obtain the experienced eSNR in case of NLOS communications.

Even though the second-order statistics of Rayleigh and Rice processes are quite different, in our case the error we make by always considering a NLOS communication is still moderate and bounded in particular situations. In fact, we are not interested in the value of eSNR but in the rate m which maximizes (31); so the error we make is located only where the best update rates for NLOS and LOS communications are different.

In Figure 7 we show the locations of the error for $\kappa = 10$. The grey areas evidence the SNR zones where we encounter errors and give an idea of the loss of SNR we face by being committed to the wrong value of m. Hence, to avoid increasing the complexity due to κ factor estimation [26, 27], the receiver can always assume a non-LOS communication and computes the channel update rate through (31).

The final receiver structure is shown in Figure 5: from the main receiver chain, demodulated symbols are passed to the extra Viterbi decoder. The output is then padded with zeros to obtain the right length for the interleaver and symbol mapper. The reconstructed OFDM symbol is then processed by the PP-MMSE algorithm which returns $\widehat{\mathbf{H}}(k)$, and the vector is stored in a circular memory buffer which saves the last m vectors $\widehat{\mathbf{H}}(k)$. The last block exploits the vehicle speed

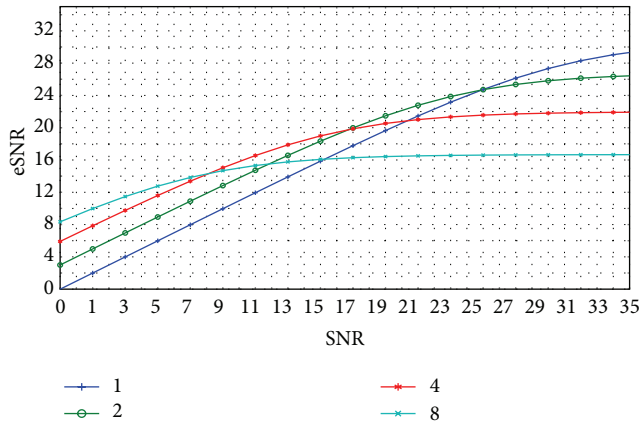

Figure 6: eSNR with respect to real SNR at a vehicle speed of 100 km/h for different channel update rates.

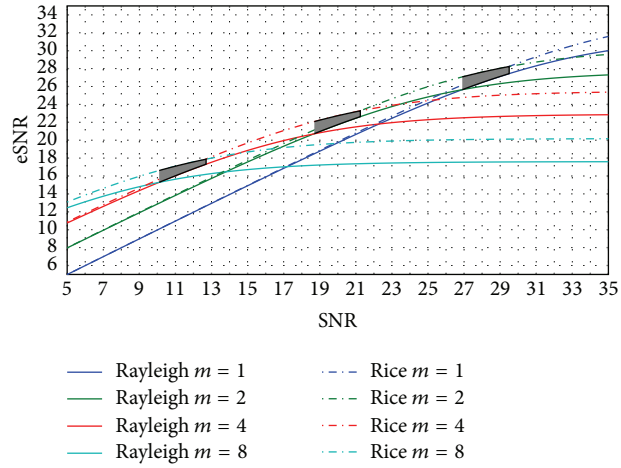

Figure 7: eSNR with respect to real SNR at a vehicle speed of 100 km/h for different channel update rates, Rice compared to Rayleigh processes.

and averages the responses and finally passes the current CR estimation to the equalizer.

5. Simulation Setup

We used the channel model implementation provided by [8]. We limited our simulations to RTV in highway scenario, considering a vehicle speed of 150 km/h.

For such a scenario, we simulated transmissions with different modulation techniques, adopting the most robust coding scheme; we build two frames with different payload lengths: the former with 200 OFDM symbols to simulate a typical IPv6 packet transmission for infotainment applications and the latter with 50 OFDM symbols to reproduce the transmission of packets for safety applications.

We compared our solution to the aforementioned receivers; we simulated as well a common WLAN receiver where no tracking technique is used. We set the STA [15] and CDP [16] parameters as suggested by the authors, in order to ensure the best performances. We assume the receivers are synchronised in both time and frequency.

The extra Viterbi decoder trellis depth has been selected to be a multiple of the inverse of all the possible coding rates to avoid problems in the zero padding process due to fractional bits. As mentioned, we have selected the longest depth that guarantees the PP-MMSE algorithm to work in every transmission scheme (17), which turns out to be 18. We set the available channel update rates to include at most 8 symbols since a higher rate does not show relevant improvements, while costing more in terms of memory. We also pruned the set to be $\{1, 2, 4, 8\}$ to simplify averaging operations. To highlight the improvement given by the speed data exploitation, we also simulated the receiver performance without the averaging step, that is, removing the channel storage block showed in Figure 5.

6. Results

As a first note, in Figures 8, 9, and 10 we can see that the classical WLANs receiver does not work in the VANET environment, no matter the choice of the modulation or SNR level.

In Figure 8 packet error rates (PER) results with BPSK modulation are shown; in this case the proposed receiver and the PP-MMSE receiver show very poor performances compared to others: this happens because of the channel estimation block. This particular transmission scheme provides only few valid subcarrier indexes, 12 indexes, worsening the performances of the PP-MMSE channel estimator; in this case the only possible solution would be to shorten the depth of the Viterbi decoder; however we think that the reward of improving the results in this scenario is not worth the deterioration we would have in all other modulation schemes.

The up-and-down slope of the proposed scheme in both Figures 8(a) and 8(b) happens exactly at the point where the channel averaging rate changes from the current level to the next one, finally reaching, as expected, the same performances of the PP-MMSE receiver when the rate becomes 1.

In Figure 9, performances of the reception of QPSK-modulated frames are shown; the proposed receiver achieves the best performances. Here the Viterbi decoder provides 28 valid subcarriers per OFDM symbol, guaranteeing to the PP-MMSE algorithm enough data to compute a precise channel estimation. The PER shows the improvement due to channel averaging: the gain is about 2 dB.

Comparing Figure 9 with Figure 8 it can be noticed that the proposed receiver obtains better results with the QPSK transmission than with the BPSK one. Figure 8 shows that even the STA and CDP receivers in the BPSK scenario have worse performances than the proposed scheme with the QPSK.

In Figure 10 a 16-QAM transmission has been used; here the number of valid subcarrier indexes reaches 32, and the gap between proposed receivers and the other ones becomes greater. On the contrary the enhancement due to channel averaging keeps the same: 2 dB as the PER curve starts to decrease.

In Figures 9 and 10, improvements of the PP-MMSE algorithm in data symbols reconstruction are shown. As

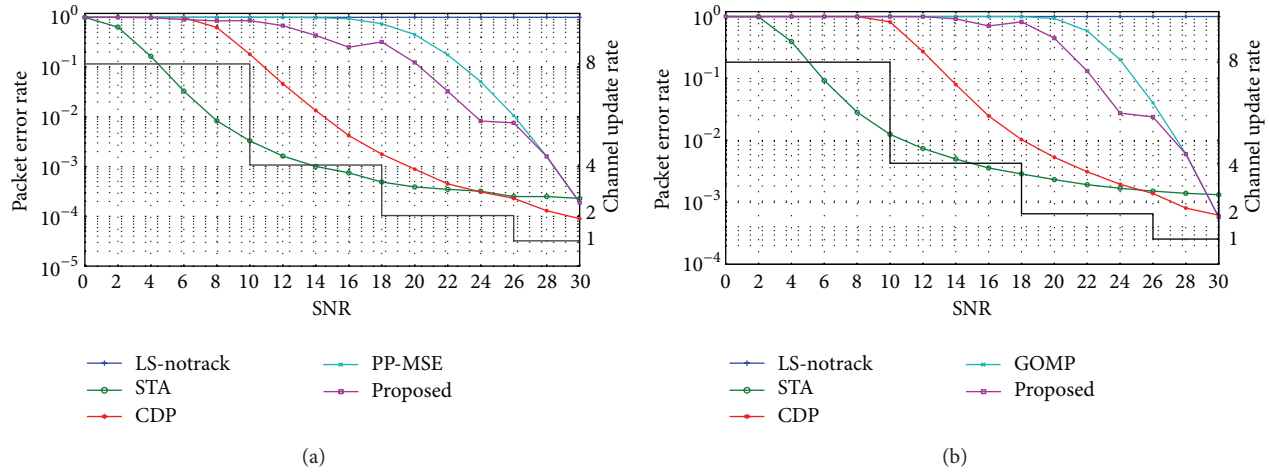

FIGURE 8: Packet error rates for (a) 50 and (b) 200 OFDM payload symbols frames; BPSK modulation is used, and the vehicle travels at 150 km/h. The piecewise constant line represents the selected channel update rates based on eSNR.

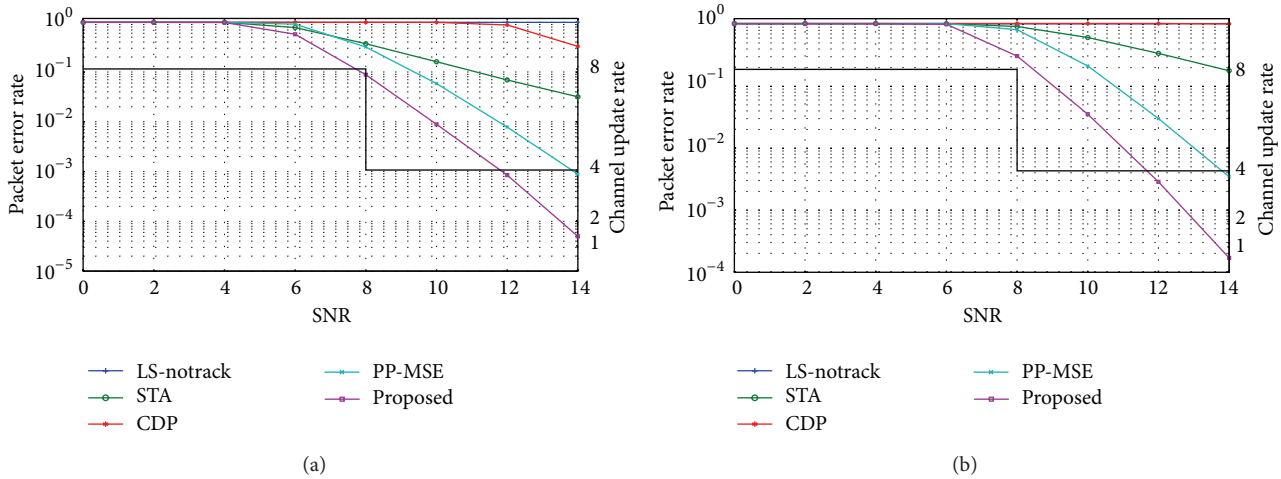

FIGURE 9: Packet error rates for (a) 50 and (b) 200 OFDM payload symbols frames; QPSK modulation is used, and the vehicle travels at 150 km/h. The piecewise constant line represents the selected channel update rates based on eSNR.

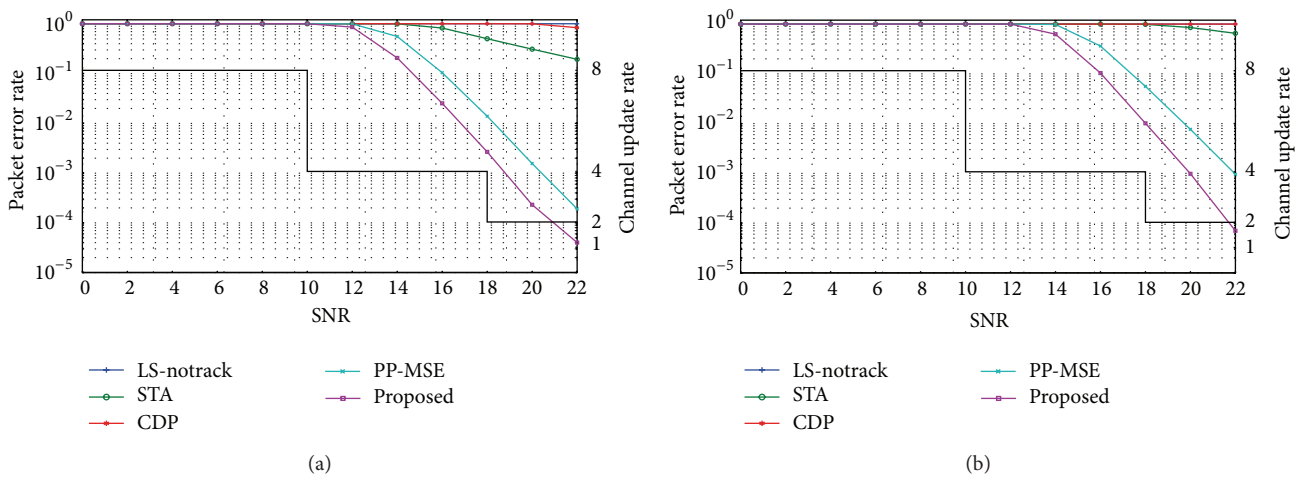

FIGURE 10: Packet error rates for (a) 50 and (b) 200 OFDM payload symbols frames; 16-QAM modulation is used, and the vehicle travels at 150 km/h. The piecewise constant line represents the selected channel update rates based on eSNR.

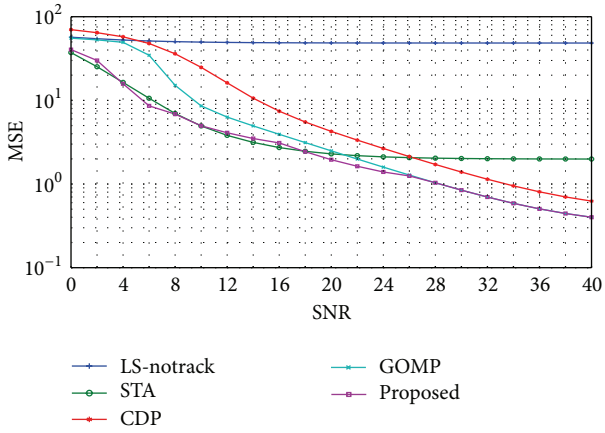

Figure 11: Channel estimation mean squared errors comparison, for the proposed receiver schemes. The transmission scheme used is QPSK with code rate 1/2 as in Figure 9(a).

previously mentioned, hard demodulation shows weakness in low SNR scenarios; by including the decoder in the channel estimation process, data-aided pseudopilot tones are less error prone. As a consequence the PER of the PP-MMSE and proposed receivers start their descending slope at lower SNR values with respect to the STA and CDP receivers.

In Figure 11 mean squared error ratios of channel estimates are compared. Since all channel estimation algorithms are based on the pseudopilot algorithm which assumes that the modulation scheme is known, the error has been computed only on frames for which the frame headers have been decoded correctly and the modulation scheme has been recognized. At low SNR values, the STA receiver performances are comparable with the ones of the proposed receivers, while, as the SNR increases, the STA receiver reaches an asymptotic value and the error gets flat. This trend compared with the PER performances seems to conflict; the cause may lie in the averaging process of the channel estimator: even if the channel estimation shows robustness to symbol errors in case of low SNR, it bounds the performances in case of high SNR values where channel variability is predominant.

7. Conclusion and Future Work

A new receiver scheme for VANETs devices has been proposed; in particular we focused on the channel response estimator which plays an essential role in the overall receiver performances in terms of bit error rate and packet error rate. We compared our solution to previous works using a well established and widely used channel model.

We showed a novel approach, in which information taken from external sensors is used to improve the receiver efficiency. We focused on a specific scenario, the RTV, where channel variance and Doppler effects are strictly connected to vehicle speed. The RTV scenario pays an important role in vehicular networks, especially regarding safety. Improving receiver performances in such a scenario means warning drivers more in advance, providing more time to react to dangers. We simulated different transmission rates and demonstrated that the channel update rate must be chosen based on the Doppler spread and not on the modulation technique as previous proposals have done.

In the future we aim to exploit these extra data to gather information useful in every environment, always keeping the focus on the highways scenario where channel variability is more relevant.

Conflict of Interests

The authors declare that there is no conflict of interests regarding the publication of this paper.

References

[1] "IEEE standard for information technology-local and metropolitan area networks-specific requirements—part 11: wireless lan medium access control (MAC) and physical layer (PHY) specifications amendment 6: wireless access in vehicular environments," IEEE Std 802.11p- 2010 (Amendment to IEEE Std 802.11-2007 as amended by IEEE Std 802.11k-2008, IEEE Std 802.11r-2008, IEEE Std 802.11y-2008, IEEE Std 802.11n-2009, and IEEE Std 802.11w-2009), pp. 1–51, 15 2010.

[2] IEEE, *IEEE Standard for Information Technology-Telecommunications and Information Exchange between Systems Local and Metropolitan Area Networks-Specific Requirements Part 11: Wireless LAN Medium Access Control (MAC) and Physical Layer (PHY) Specifications: IEEE P802.11-REVmb/D12, November 2011 (Revision of IEEE Std 802.11-2007, as Amended by IEEEs 802.11k 2008, 802.11r-2008, 802.11y- 2008, 802.11w-2009, 802.11n-2009, 802.11p-2010, 802.11z-2010, 802.11v-2011, 802.11u-2011, and 802.11s-2011)*, 2011.

[3] H. Abdulhamid, K. E. Tepe, and E. Abdel-Raheem, "Performance of DSRC systems using conventional channel estimation at high velocities," *AEU—International Journal of Electronics and Communications*, vol. 61, no. 8, pp. 556–561, 2007.

[4] M. Wellens, B. Westphal, and P. Mähönen, "Performance evaluation of IEEE 802.11-based WLANs in vehicular scenarios," in *Proceedings of the IEEE 65th Vehicular Technology Conference—VTC2007-Spring*, pp. 1167–1171, Dublin, Ireland, April 2007.

[5] N. Benvenuto and G. Cherubini, "Orthogonal frequency division multiplexing," in *Algorithms for Communications Systems and Their Applications*, chapter 9, John Wiley & Sons, Chichester, UK, 2002.

[6] J. Karedal, F. Tufvesson, N. Czink et al., "A geometry-based stochastic MIMO model for vehicle-to-vehicle communications," *IEEE Transactions on Wireless Communications*, vol. 8, no. 7, pp. 3646–3657, 2009.

[7] G. Acosta-Marum and M. A. Ingram, "Six time- and frequency—elective empirical channel models for vehicular wireless LANs," *IEEE Vehicular Technology Magazine*, vol. 2, no. 4, pp. 4–11, 2007.

[8] http://sourceforge.net/projects/physlayersim/.

[9] http://itpp.sourceforge.net/.

[10] S. I. Kim, H. S. Oh, and H.-K. Choi, "Mid-amble aided OFDM performance analysis in high mobility vehicular channel," in *Proceedings of the IEEE Intelligent Vehicles Symposium*, pp. 751–754, IEEE, June 2008.

[11] Y. Zhang, I. L. Tan, C. Chun, K. Laberteaux, and A. Bahai, "A differential OFDM approach to coherence time mitigation in

DSRC," in *Proceedings of the 5th ACM International Workshop on VehiculAr Inter-NETworking (VANET '08)*, pp. 1–6, ACM, September 2008.

[12] T. Zemen, L. Bernadó, N. Czink, and A. F. Molisch, "Iterative time-variant channel estimation for 802.11p using generalized discrete prolate spheroidal sequences," *IEEE Transactions on Vehicular Technology*, vol. 61, no. 3, pp. 1222–1233, 2012.

[13] L. R. Bahl, J. Cocke, F. Jelinek, and J. Raviv, "Optimal decoding of linear codes for minimizing symbol error rate," *IEEE Transactions on Information Theory*, vol. 20, no. 2, pp. 284–287, 1974.

[14] A. Bourdoux, H. Cappelle, and A. Dejonghe, "Channel tracking for fast time-varying channels in IEEE802.11p systems," in *Proceedings of the Global Telecommunications Conference (GLOBECOM '11)*, pp. 1–6, IEEE, Houston, Tex, USA, December 2011.

[15] J. A. Fernandez, K. Borries, L. Cheng, B. V. K. Vijaya Kumar, D. D. Stancil, and F. Bai, "Performance of the 802.11p physical layer in vehicle-to-vehicle environments," *IEEE Transactions on Vehicular Technology*, vol. 61, no. 1, pp. 3–14, 2012.

[16] Z. Zhao, X. Cheng, M. Wen, B. Jiao, and C.-X. Wang, "Channel estimation schemes for IEEE 802.11p standard," *IEEE Intelligent Transportation Systems Magazine*, vol. 5, no. 4, pp. 38–49, 2013.

[17] C.-J. Wu and D. Lin, "Sparse channel estimation for ofdm transmission based on representative subspace fitting," in *Proceedings of the IEEE 61st Vehicular Technology Conference (VTC '05)*, vol. 1, pp. 495–499, May 2005.

[18] B. Yang, K. B. Letaief, R. S. Cheng, and Z. Cao, "Channel estimation for OFDM transmission in multipath fading channels based on parametric channel modeling," *IEEE Transactions on Communications*, vol. 49, no. 3, pp. 467–479, 2001.

[19] A. F. Molisch, F. Tufvesson, J. Karedal, and C. F. Mecklenbräuker, "A survey on vehicle-to-vehicle propagation channels," *IEEE Wireless Communications*, vol. 16, no. 6, pp. 12–22, 2009.

[20] T. Abbas, L. Bernado, A. Thiel, C. Mecklenbrauker, and F. Tufvesson, "Radio channel properties for vehicular communication: merging lanes versus urban intersections," *IEEE Vehicular Technology Magazine*, vol. 8, no. 4, pp. 27–34, 2013.

[21] T. Hastie, R. Tibshirani, and J. Friedman, *The Elements of Statistical Learning*, Springer Series in Statistics, Springer, New York, NY, USA, 2001.

[22] A. Molisch, *Wireless Communications*, Wiley-IEEE Press, 2005.

[23] M. Siti, A. Agnoletto, and A. Assalini, "Doppler spread estimation and channel update period tuning in OFDM-based vehicular communication systems," in *Proceedings of the IEEE 73rd Vehicular Technology Conference (VTC '11)*, pp. 1–5, May 2011.

[24] G. Ren, Y. Chang, and H. Zhang, "SNR estimation algorithm based on the preamble for wireless OFDM systems in frequency selective channels," *IEEE Transactions on Communications*, vol. 57, no. 8, pp. 965–974, 2008.

[25] A. Abdi, J. A. Barger, and M. Kaveh, "A parametric model for the distribution of the angle of arrival and the associated correlation function and power spectrum at the mobile station," *IEEE Transactions on Vehicular Technology*, vol. 51, no. 3, pp. 425–434, 2002.

[26] A. Doukas and G. Kalivas, "Rician k factor estimation for wireless communication systems," in *Proceedings of the International Conference on Wireless and Mobile Communications (ICWMC '06)*, p. 69, July 2006.

[27] G. Azemi, B. Senadji, and B. Boashash, "Ricean K-factor estimation in mobile communication systems," *IEEE Communications Letters*, vol. 8, no. 10, pp. 617–619, 2004.